Anions formed by perchlorofluorobenzenes $C_6Cl_nF_{6-n}$ $(n = 0 - 6)$.

Thomas Sommerfeld*

Department of Chemistry and Physics, Southeastern Louisiana University, SLU 10878, Hammond, LA 70402, USA

E-mail: Thomas.Sommerfeld@selu.edu

Abstract

Anions formed by the perhalobenzene series $C_6Cl_nF_{6-n}$ $(n = 0 - 6)$ are studied computationally. All members of the series form both stable valence and stable non-valence anions. At the geometry of the neutral parents, only non-valence anions are bound, and the respective vertical electron affinities show values in the 20 to 60meV range. Valence anions show distorted non-planar structures, and one can distinguish two types of conformers. A-type conformers show puckered-ring structures and excess electrons delocalized over several C-Cl bonds [in case of $C_6F_6^-$, C-F bonds], while B-type conformers possess excess electrons essentially localized in a single C-Cl bond, which is accordingly strongly stretched and bent out-of-plane. For a specific anion, all conformers are close in energy (relative energies of less than 10kJ/mol) and are connected by low-lying transition states. Accordingly, A-type and B-type conformers possess similar adiabatic electron affinities, however, their vertical detachment energies exhibit drastically different values, which should ease conformer distinction in photoelectron spectroscopy.

1 Introduction

Small organic molecules such as ethylene, butadiene, benzene, or phenol normally cannot bind excess electrons permanently, but form only temporary anions.[1–3] Exceptions occur in the presence of at least one strongly electron-withdrawing group, that is, a group with strong negative inductive (-I) and negative mesomeric (-M) effects. For example, acetaldehyde forms a dipole-bound anion,[4–6] nitromethane forms both a dipole-bound and a valence anion,[7,8] and para-benzoquinone forms a stable valence state.[9]

In comparison with NO_2 or CHO groups, halogen atoms possess far weaker electron-drawing properties: Halogen atoms show smaller -I effects, and, in contrast to NO_2 or CHO, a positive mesomeric (+M) effect. Consequently, several halogen substituents are needed to support bound anion states. For example, only trichloromethane and tetrachloromethane form stable anions—chloromethane and dichloromethane do not.[10] The same is true considering ethene: Chloroethene does not form stable anions, and only the ipso substituted dichloromethane possess a positive electron affinity.[11] Comparing fluorine and chlorine, known electron affinities suggest that chlorine substituents promote anion formation more strongly than fluorine substituents. For example hexachlorobenzene possesses an electron affinity roughly twice as large as hexafluorobenzene.[11,12] Another, perhaps more striking example is CCl_4, which shows an electron affinity of about 0.8eV,[10] while CF_4 forms only temporary anions.[13]

In a combined experimental and theoretical study, we recently considered anion formation trends in the fluorobenzene series

$C_6H_{6-n}F_n$,[14–16] and our studies show that C_6F_6 is an outlier of both the $C_6H_{6-n}F_n^-$ ($n = 0-6$) and the C_6F_5X (X = F, Cl, Br, I) series. On the one hand, the $[O_2{\cdot}C_6F_6]^-$ photoelectron spectrum was found to be shifted to substantially higher electron-binding energies than the $n \leq 5$ spectra suggesting much stronger interactions and charge delocalization between O_2^- and C_6F_6.[14] On the other hand, the excess electron of C_6F_6 shows a delocalized binding motif, while for X = Cl, Br, I, the excess electron localizes in the C-X bonds.[17,18]

Here we extend our work by systematically replacing all F atoms of C_6F_6 by Cl, in other words, we investigate the perchlorofluorobenzene $C_6Cl_nF_{6-n}$ series with a focus on trends in anion structures and electron-binding properties. Four members of the $C_6Cl_nF_{6-n}^-$ series have been considered previously. The hexafluorobenzene anion received most attention and was studied by many different means (see e.g.[12,16,19–22]). Let us emphasize the varied history of electron affinity measurements described in Ref. [12] and the interaction between its valence and its non-valence states described in Ref. [20] The valence electron affinity of C_6Cl_6 was investigated experimentally[23] and theoretically[19] , and its non-valence state was examined in Ref. [24] Electron binding to chloropentafluorobenzene and its bromo and iodo analogs was studied in solution and in the gas phase,[17,18,25] and the branching ratio between thermal electron attachment and various dissociative attachment reactions was measured for chloropentafluorobenzene and 1,3-dichlorotetraflurobenzene.[26]

The paper is organized as follows: Section 2 describes the theoretical approaches employed. Method-related results as well as trends regarding anion structures, vertical electron affinities, adiabatic electron affinities, and vertical detachment energies are presented in section 3. Section 4 summarizes our results and discusses their impact in the light of photoelectron spectroscopy.

2 Theoretical Methods

We follow mainly the computational protocols established in ref.[15] Minimal energy structures of 13 neutral $C_6Cl_nF_{6-n}^-$ compounds and their associated anions are identified using the density functional (DF) methods ωB97X[27] (a range-separated hybrid functional) and B2GPLYP[28] (a double hybrid functional) in combination with the Ahlrichs def2-TZVPPD basis set.[29] For all minima, vibrational frequencies were computed using both DFs, while electrostatic properties of the neutral compounds (dipole and quadrupole moments) were computed only with the ωB97X DF.

Anions of several $C_6Cl_nF_{6-n}^-$ halobenzenes possess two or more conformers. For several prototypical cases, the minimal energy path (MEP) connecting the conformer structures was computed using the nudged elastic band (NEB) method,[30] which yields a set of structures (images) along the MEP. Transition states were then optimized starting from the highest image, and the nature of the predicted transition states was confirmed by computing vibrational frequencies.

At a fundamental level, the electron binding properties of a molecular system can be characterized by three values: The vertical electron affinity (VEA) of the neutral, the vertical detachment energy (VDE) of the anion, and the adiabatic electron affinity (AEA) (see Fig. 1). The VEA is the energy difference between anion and neutral evaluated at the geometry of the neutral. A positive VEA indicates that the anion can bind an electron without geometry distortion, a negative VEA refers to so-called temporary anions or resonance states, which require special methods.[31,32] The VDE is the same energy difference, however, evaluated at the geometry of the anion (Fig. 1). A positive VDE implies that the anion is at least locally bound, while a negative VDE again indicates a resonance state. For a bound anion, the VDE is loosely related to the peak of the photoelectron signal through the Franck-Condon principle. Last, the AEA is yet again the energy difference between anion and neutral, but both neutral and anion energy are evaluated

at their respective minimum energy structures (Fig. 1). In this context, it is understood that two *related* minimal energy structures are considered in the sense that adiabatic relaxation of a detached anion would lead to the neutral structure. This energy corresponds in principle to the onset of the photoelectron signal, while the practical onset is impacted by the intensities of the low-energy transitions in comparison with the background level. Alternatively, the AEA can be defined as the difference between the most stable neutral and most stable anion structures, but this definition may lead to unrelated minima and therefore experimentally irrelevant AEA values.

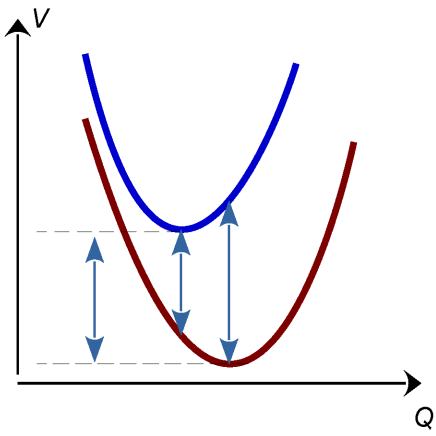

Figure 1: Schematic potential energy curves of a neutral (dark blue) and its associated anion (maroon), where Q is a coordinate connecting the minima of the neutral and the anion. The arrows represent—from left to right—the AEA, the VEA, and the VDE (without zero-point corrections). The schematic curves shown correspond to a neutral possessing strongly electron-withdrawing groups so that both the VEA and the AEA are positive (see text).

The VEA of small organic molecules is normally negative, indicating that occupation of the lowest unoccupied valance orbital yields an unstable temporary state. Exceptions occur if several strongly electron-withdrawing groups are present, for example, for nitrates or quinones, but the chlorofluorobenzene molecules considered here are no exception from this trend. Still, all halobenzenes considered form stable non-valence states with VEAs in the 10 to 100 meV range. These states have already been characterized for $C_6F_6^-$ and $C_6Cl_6^-$ (see refs[20,24]), and to establish trends, we compute the non-valence VEA of all 13 neutral $C_6Cl_nF_{6-n}^-$ compounds using the third-order algebraic diagrammatic construction method (ADC(3)) and the aug-cc-pVTZ basis set augmented with a (7s7p7d) set of diffuse functions located at the center of the six-membered ring (l-independent even-tempered exponents between 0.05 and 0.00001221; even-scaling factor 4).

In contrast to the VEA, the VDE and AEA values are all associated with valence states. Thus, on the one hand, VDEs and AEAs can be directly calculated from the ωB97X and B2GPLYP total energies. On the other hand, we have computed VDEs and AEAs from single-point energies obtained from domain-based local-pair natural-orbital coupled-cluster calculations with single, double, and non-iterative triple substitutions (DLPNO-CCSD(T)).[33] In the DLPNO-CCSD(T) computations, tight thresholds were applied for all cutoff parameters: 10^{-7} for the pair natural-orbital (PNP) occupation number cutoff, 10^{-5} for the estimated pair correlation energy cutoff, $5 \cdot 10^{-3}$ for the PNO domain construction cutoff, and 10^{-3} for a cutoff controlling the local fit (see the manual of the ORCA package[34,35]). While VDEs are straightforward differences of electronic energies, zero-point energy (ZPE) corrections have been applied to the AEA values using either ωB97X or B2GPLYP ZPEs as appropriate for the considered geometries. We note that this computational protocol doesn't yield benchmark electron affinities, but comparison with known experimental electron affinities shows that the predicted values can be expected to slightly underestimate VDEs and AEAs by between 0.1eV and 0.2eV. However, trends along the $C_6Cl_nF_{6-n}^-$ series are expected to be reproduced faithfully.

The Q-Chem package[36] (version 6.0.1) was used for ADC(3) computations; all other computations have been performed with the ORCA package of programs (version 5.0.4).[34]

3 Results and Discussion

In this section we consider anions formed by the $C_6Cl_nF_{6-n}$ series of halobenzene compounds with special emphasis on anion structures and trends in the electron binding properties. Regarding the neutral halobenzenes, for $n = 0, 1, 5$, and 6 chlorine atoms, only a single isomer exists. In contrast, for each of $n = 2, 3$, and 4, there are three isomers, leading to a total of 13 different $C_6Cl_nF_{6-n}^-$ compounds. The geometrical structures of these compounds and the numbering scheme used in this article are shown in Fig. 2. All neutral molecules are planar and show symmetries consistent with their substitution pattern (geometries are supplied in the SI).

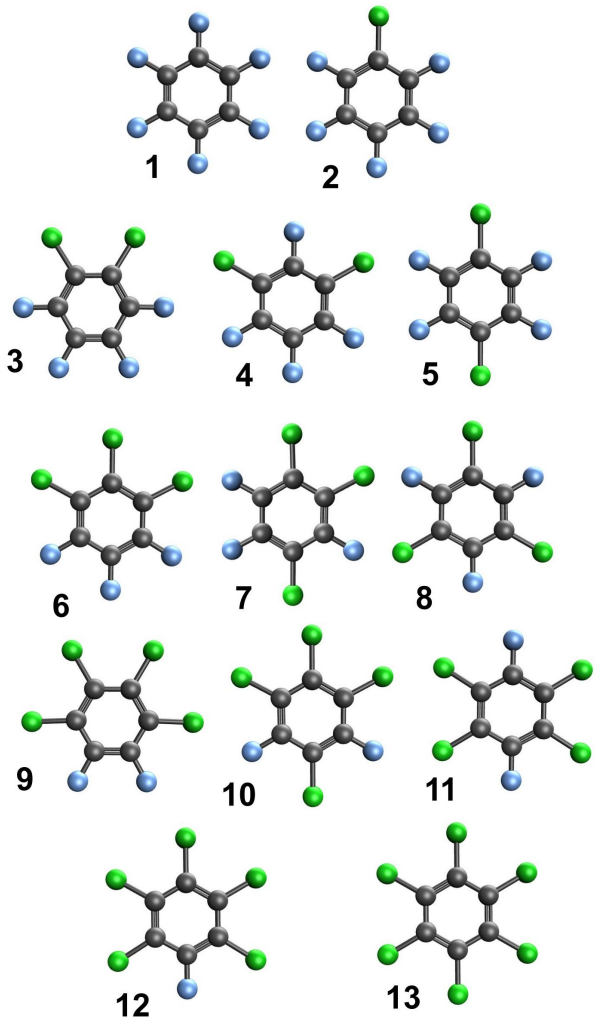

Figure 2: Geometrical structure and numbering scheme of 13 $C_6Cl_nF_{6-n}$ halobenzene compounds. Fluorine and chlorine atoms are indicated as blue and green balls.

Before considering electron binding properties and anion structures in detail, let us briefly discuss methods-related results. All presented electron affinities and relative energies depend on density functional geometry optimizations. On the one hand, density functional geometries are used to evaluate DLPNO-CCSD(T) single-point energies, on the other hand, density functional frequencies are used to compute ZPEs. In general, both functionals, ωB97X and B2GPLYP, predict very similar geometries, in particular, very similar C-C and C-F bond lengths. ZPEs also differ by a few percent at most. However, in comparison with ωB97X, B2GPLYP predicts somewhat different C-Cl bond lengths: In general, B2GPLYP predicts slightly longer C–Cl bonds than ωB97X (differences of a few thousandths of an Å), however, in anion conformers exhibiting electron localization in a single C–Cl bond, the opposite is true, and for these C-Cl bonds B2GPLYP predicts distinctly shorter lengths than ωB97X (differences of several hundredths of an Å).

The quality of these geometries can be evaluated by comparing the associated DLPNO-CCSD(T) single point energies. For all neutral halobenzenes, DLPNO-CCSD(T) energies are slightly lower at the B2GPLYP geometries (differences of up to 1.4kJ/mol) indicating that the the DLPNO-CCSD(T) structures are closer to B2GPLYP structures than to ωB97X structures. With the single exception of the $C_6F_6^-$ anion, the same is true for halobenzene anions (slightly larger differences of up to 4kJ/mol).

In comparison with VDEs and AEAs, these energy differences are negligible, and it does not matter which geometry is used to evaluate electron binding properties. Yet, relative energies of anion conformers show magnitudes of a few kJ/mol (10kJ/mol or less; see below), and consequently differences in the kJ/mol order become relevant. We therefore present B2GPLYP geometries and results obtained at these structures.

A second methodological issue arises in the context of ZPE corrections. Since anions normally show much looser structures than their neutral parents, ZPE corrections of AEAs can be sustantial (here about 0.1eV). ZPE correc-

tions of relative energies of anion conformers tend to be considerably smaller (a few kJ/mol), because two anion structures are compared, which possess identical numbers of electrons occupying bonding and antibonding orbitals, respectively, and therefore somewhat lower vibrational frequencies than the parent neutral. However, relative conformer energies are much smaller than AEAs, and their ZPE corrections have the same order of magnitude as the relative energies themselves. Note that conformer energy ordering is independent of zero-point corrections, but we found one transition state for which ZPE correction leads to unphysical results. We attribute this behavior to the harmonic approximation, because anharmonicities of low energy puckering modes and modes involving strongly stretched C–Cl bonds can be expected to be substantial (c.f.[18]). Thus, in the context of transition states connecting anion conformers, we present uncorrected energies and focus instead on the vibrational frequencies associated with the normal modes closely corresponding to the MEP. The harmonic ZPEs of these particular modes provide an upper bound for the true ZPEs along the minimal energy pathway and can be compared to the barriers in a meaningful way.

Regarding electron binding properties of the 13 members of the $C_6Cl_nF_{6-n}$ series, we start with the VEA. As normal for organic molecules in this size range, the 13 compounds do not form stable valence anions at the geometric structures of the neutrals—at these geometries, all valence anions are resonances with finite lifetimes. However, all 13 $C_6Cl_nF_{6-n}$ molecules form Rydberg-like non-valence anions with electron binding energies in the 20 to 60 meV range. For C_6F_6 ($n = 0$) and C_6Cl_6 ($n = 6$), these anions have previously been characterized[20,24] as correlation-bound states.[37,38] In other words, electron-correlation is needed to predict a positive VEA; taking into account electrostatic interactions at the self-consistent field level is insufficient.

The non-valence VEA for all 13 $C_6Cl_nF_{6-n}$ halobenzenes is shown in Fig. 3 together with the electrostatic properties of each compound. (A table of VEAs is supplied in the SI.) With

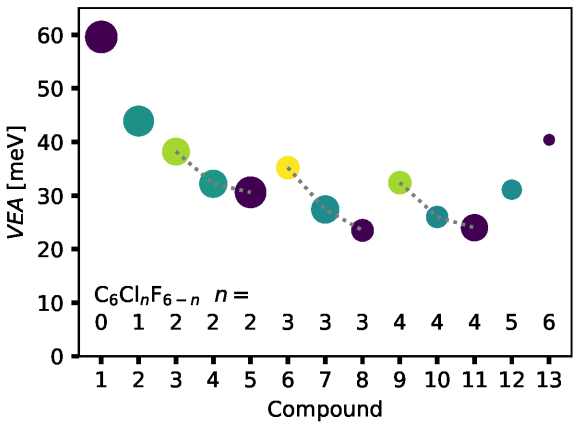

Figure 3: VEA of 13 $C_6Cl_nF_{6-n}$ halobenzenes. Compound numbers are defined in Fig. 2, and in addition the number n of chlorine atoms is indicated. VEA values for isomers with common n have been connected to guide the eye. Symbol color indicates dipole moments (purple: 0 D; turquoise: 0.25 to 0.29 D; green: 0.48 D; and yellow: 0.55 D), while symbol size indicates quadrupole moment norms (see text): 2.5 DÅ for C_6Cl_6 (compound **13**) to 27 DÅ for C_6F_6 (compound **1**).

60meV, C_6F_6 exhibits the largest VEA, while the VEAs of Cl-containing compounds vary noisily between 25 and 45meV. Often, it is possible to relate non-valence VEAs of a class of similar compounds to the multipole moments or their polarizabilities,[2,6,39–43] but the series of $C_6Cl_nF_{6-n}$ seems to lack any strong relationship of that kind. In comparison with typical moments of dipole-bound state [dipoles in excess of 2.5 D] or quadrupole-bound states [moments in the order of 50 DÅ], the 13 halobenzenes possess only small dipole and quadrupole moments. Dipole moments range from 0 to 0.55 D (Fig. 3). Quadrupole moments are characterized by a trace-less symmetric tensor, and symbol size in Fig. 3 corresponds to the Frobenius norm of this tensor (c.f.[44]), which ranges from 2.5 DÅ for C_6Cl_6 to 27 DÅ for C_6F_6. As Fig. 3 shows, neither dipole nor quadrupole moments nor their combination can serve as a predictors for the VEAs of all considered halocarbons. Dipole moments show a limited relation with VEA in the sense that for a common number of chlorine substituents (regioiso-

mers), higher dipoles correspond to higher VEA (see connected triples in Fig. 3). In contrast, quadrupoles seem essentially unrelated to VEA even in related groups of compounds. For example, C_6F_6 shows the largest quadrupole norm and the largest VEA, but the quadrupole norm of all Cl containing compounds (**2** to **13**) varies considerably, while the associated VEAs remain fairly constant (35 to 45 meV). Moreover, for Cl containing compounds, large quadrupoles tend to be associated with relatively low VEAs. Last, isotropic polarizabilities show the same lack of relation to VEA: The isotropic polarizability grows linearly with the number of Cl substituents from 483$\mathring{A}^3$ for C_6F_6 to 1045$\mathring{A}^3$ for C_6Cl_6, while the VEA shows no relationship with the Cl number.

Let us turn to valence anions of the considered halobenzenes. All valence anions represent temporary states at the geometry of their neutral parents (see above); however, at their own minimal energy structures, all neutrals form at least one stable anion. $C_6F_6^-$ is known to possess a puckered C_{2v} symmetrical structure where the excess electron is best characterized as delocalized in antibonding C–F σ^* orbitals.[45] Halobenzenes with at least one Cl substituent ($n \geq 1$) also form stable valence anions, but for these systems the excess electron prefers to occupy C–Cl antibonding orbitals, and Cl-substituted anions may form multiple stable conformers. (See SI for structures of all anion conformers.) One can distinguish two types of valence anion conformers. A-type conformers are similar to $C_6F_6^-$—which can be considered an A-type analog anion—in that the excess electron is delocalized over several C–Cl bonds. In comparison with their neutral parents, C–Cl bonds are somewhat elongated, and A-type anions show puckered structures (see Fig. 4 for a typical example). In contrast, in B-type conformers, the electron is localized in the antibonding orbital of a specific C–Cl bond. Consequently, the C–Cl bond in question is strongly elongated and only a single Cl atom is strongly bent out of plane (see Fig. 4). B-type conformers can be said to possess so-called three-electron bonds:[46] Two electrons occupy a bonding σ orbital and one electron occupies the associated anti-bonding σ^* orbital, which reduces the bond-order to 1/2.

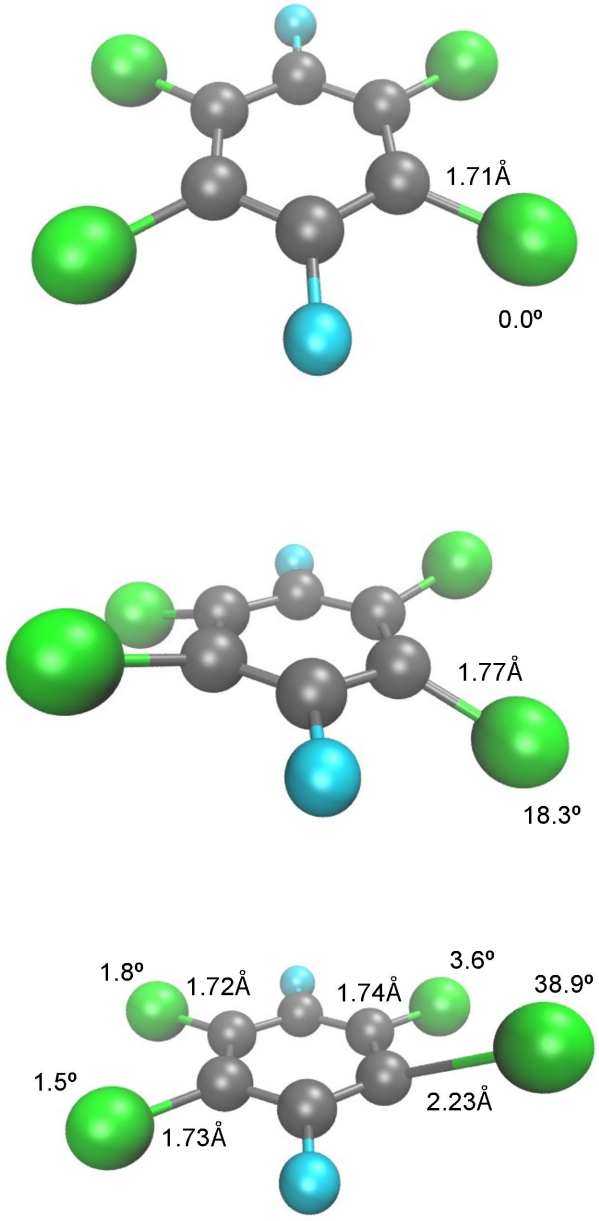

Figure 4: Structures of neutral halobenzene **11** $C_6Cl_4F_2$ (top) and its A-type (middle) and B-type (bottom) anions. The bond lengths of all symmetry-unique C-Cl bonds and the angles of the these bonds with respect to the plane of the ring are indicated.

All Cl containing $C_6Cl_nF_{6-n}$ ($n \geq 1$) compounds form one or more B-type conformers, one for each symmetry-unique Cl atom. For example, halobenzene **7** possesses three symmetry-distinct Cl atoms and consequently forms three B-type anion conformers. A-type

conformers are less common: Compounds **6**, **7**, **9**, **10**, **11**, **12** and **13** form A-type anion structures. It seems several adjacent Cl atoms are required to form stable A-type structures. The relative stability of all A and B-type conformers is displayed in Fig. 5. Owing to its lack of Cl substituents, $C_6F_6^-$ can neither form A nor B-type conformers, however, since it shows a puckered structure and its excess electron is delocalized over all C–F bonds, we group it with the A-type anions. Regarding Cl-containing $C_6Cl_nF_{6-n}^-$ ($n \geq 1$) anions, A-type and B-type conformers show very similar energies with differences of less than 10kJ/mol. For example, CCl_5F^- forms an A-type and three B-type conformers. The A-type conformer is most stable, but the three B-type conformers are only 1.8, 3.1, and 5.8kJ/mol higher in energy. As a general trend, B-type conformers are slightly more stable for conformers with $n \leq 4$, while A-type conformers represent the most stable structures for $n = 5$ and 6.

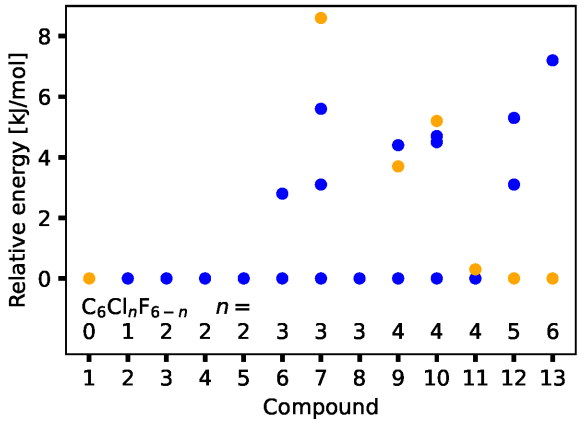

Figure 5: Relative energies of all anion minima associated with the 13 $C_6Cl_nF_{6-n}$ halobenzenes shown in Fig. 2. For each compound, the energy of the most stable anion structure is chosen as origin. A and B-type minima are indicated by orange and blue symbols, respectively. Data computed from zero-point corrected B2GPLYP absolute energies.

Since there are only minor energy differences between related anion conformers, and since these conformers are converted by simple stretching and bending motions, one may expect low-lying transition states for conformer interconversion. We investigated six examples (Tab. 1): The A-type to B-type interconversions of **9**, **11** and **13** as well as the B-type to B-type interconversions of **6** and **9**.

Table 1: Interconversion barriers between anion conformers of halobenzenes **6** (1,2,3-trichloro-4,5,6-trifluorobenzene), **9** (1,2,3,4-tetrachloro-5,6-difluorobenzene), **11** (1,2,4,5-tetrachloro-3,6-difluorobenzene), and **13** (hexachlorobenzene) computed with the NEB method at the B2GPLYP level. The E_e values given are relative energies (in kJ/mol) of both conformers and their connecting transition state. For comparison, the harmonic zero-point energies of the modes most closely associated with the minimum energy pathway E_p (in kJ/mol) are listed (see text). The anion of **9** possesses two B-type conformers with either the C(1)-Cl (B-1) or the C(2)-Cl (B-2) bond being stretched.

compound	reactant conformer			transition state	prod
	type	E_e	E_p	E_e	type
6	B	0.0	0.97	19	B
9	A	6.5	1.9	19	B-1
9	A	6.5	1.9	13	B-2
9	B	0.0	0.91	19	B
11	A	2.8	2.3	6.2	B
13	A	0.0	2.4	6.4	B

The two investigated B-type to B-type conversions are very similar to the rotation barrier of the central bond of butane. The two minima show energy differences of about 4kJ/mol—similar to the energy difference of gauche and anti butane—and the separating barrier translates into activation energies of about 20 and 15kJ/mol above the most stable conformer—very similar to the eclipsed conformations of butane (Tab. 1). For both B-type to B-type conversions studied, the transition states b some similarity with A-type conformers in that the excess electron is delocalized over two elongated C–Cl bonds, but the transition states lack the strong puckering of A-type conformers. Owing to the small barrier heights, rapid conformer interconversion can be expected at temperatures as low as 150K.

The barriers of the investigated A-type to B-type conversions decrease with increasing number of Cl-substituents. The anion of **9** possesses an A-type and two B-type conformers, and the activation energies for the A-type to B-type interconversions show values between 19 and 6.5kJ/mol. For the anions of **11** and **13** the barriers are considerably smaller, even smaller than the rotational barrier in ethane: For the anion of halobenzene **11** the barrier translates into activation energies of 3.4 and 6.2kJ/mol, respectively, and for the anion of **13** the activation energies are 6.4 and 1.6kJ/mol. In particular the latter activation energy possesses the same order of magnitude as the vibrational spacing of the modes connecting the minima, and in the harmonic approximation the B-type conformer supports only a single vibrational state. Thus, at 0K the B-type anion of **13** effectively represents a stable species, but even at temperatures as low as 100K, $C_6Cl_6^-$ can be considered to have a floppy structure.

Having characterized the anions formed by the halobenzenes $C_6Cl_nF_{6-n}$, we now turn to their AEAs. An overview displaying the AEA of all anion conformers can be found in Fig. 6, and all AEAs are listed in the SI. B-type conformers are more abundant and possess—practically independent of Cl-number n—AEAs in the 0.69 ± 0.03eV range. Clearly, the fluorine/chlorine substitution pattern in the planar ring has little impact on the local electron affinity of the stretched C–Cl bond. A-type conformers are less common and show AEAs in the same order of magnitude as B-type conformers (from 0.68 to 0.81eV). However, in contrast to the B-type conformers, A-type conformers exhibit a clear trend of increasing AEA with increasing Cl substitution that reflects the increased stability of A-type conformers with growing n (compare Figs. 5 and 6).

Last, we examine the VDE trends of the different anion conformers (Fig. 7). A-type conformers exhibit very similar VDEs in the 1.37 to 1.44eV range, a bit higher than the VDE of the related $C_6F_6^-$ anion. In contrast, B-type conformers exhibit considerably larger VDEs ranging from 2.38eV for $C_6Cl_6^-$ to 2.80eV for $C_6ClF_5^-$ (see Fig. 7 and the table provided in the SI).

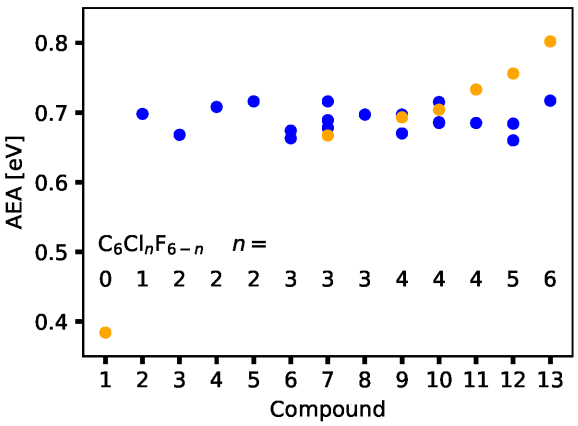

Figure 6: AEA of all anion minima associated with the 13 $C_6Cl_nF_{6-n}$ halobenzenes shown in Fig. 2. A and B-type anions are indicated by orange and blue symbols, respectively.

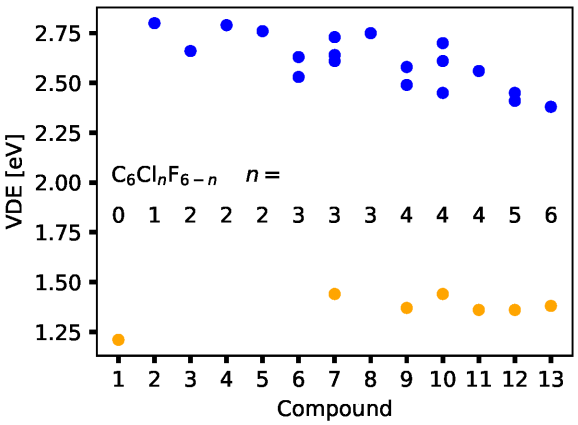

Figure 7: VDE of all anion minima associated with the 13 $C_6Cl_nF_{6-n}$ halobenzenes shown in Fig. 2. A and B-type anions are indicated by orange and blue symbols, respectively.

The VDE values of B-type conformers show a noisy trend of decreasing VDE with Cl-number n. While n itself is a poor predictor for VDE, the data can be fit surprisingly well with a simple linear model that codes the substitution pattern in relation to the strongly elongated C–Cl in which the excess electron localizes.

$$VDE = E_0 + c_o f_o + c_m f_m + c_p f_p \qquad (1)$$

Here f_o, f_m, and f_p represent the number of fluorine atoms in the ortho, meta, and para positions relative to the elongated bond, E_0 corresponds to the VDE of $C_6Cl_6^-$ within the model

(no fluorine substitution), and c_o, c_m, and c_p are regression coefficients.

Table 2: Parameter and R^2 from fitting eq.(1) to the VDEs of B-type anions. Parameter values in eV.

	OLS	LASSO
E_0	2.389	2.418
c_o	0.152	0.144
c_m	0.032	0.022
c_p	0.063	0.043
R^2	0.996	0.984

We investigated standard ordinary least squares (OLS) fitting as well as the more robust least-absolute-shrinkage-and-selection-operator (LASSO) regression. The results (R^2 and optimal parameter values) are listed in Tab. 2. Since both regressions show high R^2 values above 0.98 and the predicted parameters agree well with each other, we conclude that overfitting is not an issue. The model parameters show that any fluorine substitution tends to increase the VDE of a C–Cl bond, but fluorine atoms in the ortho position exert the greatest influence by far suggesting that the VDE variation of B-type conformers is caused by inductive effects.

4 Conclusions

Anions formed by the halobenzene series of compounds $C_6Cl_nF_{6-n}$ have been studied. All 13 neutral parents possess planar structures with symmetries reflecting the respective substitution pattern, and all neutrals form both valence and non-valence anions. The valence anions are strongly bound showing VDEs above 1eV and AEAs in the 0.4 to 0.8eV range. However, at the geometries of their neutral parents, all valence anions are unstable and represent short-lived temporary states. In contrast, non-valence states are stable at the neutral geometries, and the VEAs of the halobenzene are hence associated with non-valence states.

Before discussing our results, let us reiterate that the employed computational protocols provide good—but not benchmark—quality electron binding energies.[14] We therefore focus on trends—not on individual values. For example, comparison with the known AEAs of C_6F_6, C_6ClF_5, and C_6Cl_6 shows that the computed electron affinities of valance states are underestimated by 0.05 to 0.15eV. Since VDEs refer to the same two states, one may expect systematic errors in the same order of magnitude. VEAs, on the other hand refer to non-valance states, and the errors of the ADC(3) method are much smaller [in extreme cases going beyond ADC(3) by including triples with a method such as EOM-CCSDT may increase the computed values by 10%[38,45]]. In contrast, the employed protocol is expected to yield reliable results for the relative energy of isomers, because systems with the same number of electrons and with similar electronic structures are compared.

The non-valence VEAs of the 13 halobenzenes have been investigated with the third-order propagator method ADC(3). Typical for non-valence states of molecules without significant dipoles,[24,45] all VEAs are predicted to be smaller than 100meV. C_6F_6 possesses by far the largest VEA, while the VEAs of all Cl-containing compounds fall into the 25 to 45meV range. We tried to relate the computed VEAs to multipole moments and isotropic polarizabilities of the neutral molecules, but neither quadrupole norms nor isotropic polarizabilities seem to possess any predictive power. In contrast, dipole moments predict the order of the VEA within a family of $C_6Cl_nF_{6-n}$ isomers with common number of Cl substituents (for either $n = 2$, $n = 3$, or $n = 4$). It might be possible to develop predictive models based on quadrupole or polarizability tensors, but the current set of compounds is too small to explore this possibility. We conclude that close-range interactions with the neutral core are more important than the asymptotic molecule-electron interactions, and that non-valance anions of the $C_6Cl_nF_{6-n}$ series are best characterized as correlation-bound states.[20,24]

In addition to the weakly-bound non-valence states, all members of the $C_6Cl_nF_{6-n}$ form stable valence anions. Two types of valence anion

can be identified: A-type conformers are characterized by excess electrons delocalized over several C–Cl bonds, while B-type conformers possess excess electrons essentially localized in a single specific C–Cl bond. Accordingly, A-type anion conformers show structures with several stretched and bent out-of-plane C–Cl bonds that are closely related to low-lying puckering modes of their neutral parents. We note that the valence anion of $C_6F_6^-$ can be characterized as an A-type analog structure. In contrast, B-type anion conformers show structures with a single strongly stretched and bent out-of-plane C–Cl bond, and different B-type conformers are formed for each symmetry-unique Cl atom present. In terms of vibrational modes of their neutral parents, B-type distortions correspond to linear combinations of several stretching and puckering modes.

A-type structures require several Cl substituents, and for $n = 1 - 3$, only a single A-type conformer exists. Therefore, B-type structures represent the most stable conformers in this n-range. Halobenzenes with four Cl substituents ($n = 4$) represent a transition region with nearly degenerate A and B-type structures, and, for $n = 5, 6$, the most stable structures are A-type conformers. However, energy differences between anion conformers originating from a single neutral parent are generally tiny: Relative energies show typical values of a few kJ/mol, and all relative energies are predicted to be smaller than 10kJ/mol. In addition, all anion conformers of a given neutral can be interconverted through simple stretching and puckering motions leading to low-lying transition states with barrier heights in the same order of magnitude as rotations about C–C single bonds. At finite temperatures, conformer interconversion is hence expected to progress rapidly, and for $n \geq 4$, $C_6Cl_nF_{6-n}^-$ compounds are probably best characterized as floppy structures.

For the electron binding properties of the valence anions the following trends emerge. All Cl substituted halobenzenes show considerably larger AEAs than C_6F_6. B-type conformers generally possess AEAs of about 0.7eV, practically independent of their neutral parents—a value that can be understood as the local electron affinity of a single C–Cl bond—in other words, the particular F/Cl substitution pattern of the remaining bonds barely affects the AEA of B-type conformers. In contrast, the AEA of A-type conformers systematically increases with the number of Cl substituents; however, A-type AEAs nevertheless show values close to their B-type cousins with values ranging from 0.67 to 0.8eV. We conclude that AEAs have little value for distinguishing A and B-type conformers.

In contrast to the AEAs, VDEs of A-type and B-type conformers exhibit vastly different values and trends. A-type VDEs are close to 1.4eV—not much higher than the VDE of the A-analog $C_6F_6^-$ anion. VDEs of B-type conformers are substantially higher and show far more variation (2.4 to 2.8eV range). This variation can be reproduced by a simple linear model using as descriptors the numbers of fluorine atoms in the ortho, meta, and para positions with respect to the elongated C–Cl bond. In particular the number of ortho fluorine substituents explains the bulk of the variation, and we conclude that the differences in the VDE of a specific C–Cl bond come down to inductive effects of the neighboring substituents with fluorine possessing a larger -I effect than chlorine.

All in all, the following picture emerges from the observed trends: As a third-row atom, Cl is considerably larger and shows far lower electronegativity than F. In comparison to C–F bonds, C–Cl bonds are hence less polar, and, owing to the size difference, their σ^* orbitals have lower energies rendering C–Cl bonds much more accommodating to excess electrons.[47] Consequently, C_6F_6 plays the role of an outlier regarding all electron binding properties: It shows a considerably higher VEA, but a much lower AEA than the Cl-substituted halobenzenes. For a given chlorofluorobenzene, a competition arises between localizing the excess electron in a single C–Cl bond and delocalizing the excess electron over several C–Cl bonds. Excess electron localization and delocalization are preferred for low and high numbers of Cl substituents, respectively, but the energy differences are tiny, and the two con-

former types are connected by low barriers so that rapid conformer interchange is expected for any but the lowest temperatures.

Last, let us consider photoelectron spectroscopy of $C_6Cl_nF_{6-n}$ anions. As mentioned in the introduction, photoelectron spectra of $C_6F_6^-$ and $C_6ClF_5^-$ have been reported previously.[16,18,22] Both spectra exhibit broad, vibrationally unresolved detachment transitions, indicating that the equilibrium structures of the anions differ significantly from those of their neutrals. Moreover, in going from $C_6F_6^-$ and $C_6ClF_5^-$, the peak of the detachment spectrum, which can be loosely associated with the respective VDEs, shifts by about 1.4eV to higher energies. Both observations are consistent with our computations: The excess electrons resides in C–Cl antibonding σ^* orbitals, which explains the differences between neutral and anionic structures, and the VDE of the B-type conformer of $C_6ClF_5^-$ is predicted to be about 1.6eV higher than that of $C_6F_6^-$.

Richer detachment spectra are expected for anions possessing multiple conformers, in particular, for anions possessing both A-type and B-type conformers. Since photodetachment occurs faster than nuclear dynamics, photoelectron spectra of multi-conformer anions should in principle represent a superposition of the spectra of each conformer. Owing to the low energy-differences and low interconversion barriers, all conformers can be expected to be populated at typical experimental internal temperatures. The spectra of single conformers can, of course, be expected to be broad, but owing to the large differences in VDE of A-type and B-type conformers, one may be able to easily distinguish A-type and B-type conformers in experimental spectra. In any case, we predict conformer populations and accordingly photoelectron spectra to be strongly temperature-dependent, and hope that our predictions will not only stimulate experiments, but also aid in their interpretation.

Acknowledgement The author thanks Caroline Chick Jarrold for stimulating discussions and acknowledges support by the National Science Foundation under CHE-2303652.

Supporting Information Available

The following files are available free of charge.

- xyz.zip: Minimum-energy structures of all neutrals and anions considered.
- EA.xlsx: Spreadsheet listing all computed adiabatic electron affinities, vertical electron affinities, and vertical detachment energies.

References

(1) Jordan, K. D.; Burrow, P. D. Studies of the temporary anion states of unstaturated hydrocarbons by electron transmission spectroscopy. *Acc. Chem. Res.* **1978**, *11*, 341–348.

(2) Simons, J. Molecular anions. *J. Phys. Chem. A* **2008**, *112*, 6401.

(3) Simons, J. Molecular anions perspective. *The Journal of Physical Chemistry A* **2023**, *127*, 3940–3957.

(4) Desfrançois, C.; Abdoul-Carime, H.; Khelifa, N.; Schermann, J. P. From $\frac{1}{r}$ to $\frac{1}{r^2}$ potentials: Electron exchange between Rydberg atoms and polar molecules. *Phys. Rev. Lett.* **1994**, *73*, 2436–2439.

(5) Compton, R. N.; Hammer, N. I. Multipole-bound molecular anions. Advances in Gas-Phase Ion Chemistry. Stamford, Connecticut, 2001; pp 257–305.

(6) Jordan, K. D.; Wang, F. Theory of dipole-bound anions. *Annu. Rev. Phys. Chem.* **2003**, *54*, 367.

(7) Compton, R. N.; Carman, Jr., H. S.; Desfrançois, C.; Abdoul-Carmine, H.; Schermann, J. P.; Hendricks, J. H.; Lyapustina, S. A.; Bowen, K. H. On the binding of electrons to nitromethane: Dipole and valence bound anions. *J. Chem. Phys.* **1996**, *105*, 3472.

(8) Adams, C. L.; Schneider, H.; Ervin, K. M.; Weber, J. M. Low-energy photoelectron imaging spectroscopy of nitromethane anions: Electron affinity, vibrational features, anisotropies, and the dipole-bound state. *J. Chem. Phys.* **209**, *130*, 074307.

(9) Schiedt, J.; Weinkauf, R. Resonant photodetachment via shape and Feshbach resonances: p-benzoquinone anions as a model system. *The Journal of Chemical Physics* **1999**, *110*, 304–314.

(10) Staneke, P.; Groothuis, G.; Ingemann, S.; Nibbering, N. Formation, stability and structure of radical anions of chloroform, tetrachloromethane and fluorotrichloromethane in the gas phase. *International Journal of Mass Spectrometry and Ion Processes* **1995**, *142*, 83–93.

(11) Wiley, J.; Chen, E.; Chen, E.; Richardson, P.; Reed, W.; Wentworth, W. The determination of absolute electron affinities of chlorobenzenes, chloronaphthalenes and chlorinated biphenyls from reduction potentials. *Journal of Electroanalytical Chemistry and Interfacial Electrochemistry* **1991**, *307*, 169–182.

(12) Miller, T. M.; Van Doren, J. M.; Viggiano, A. Electron attachment and detachment: C_6F_6. *International Journal of Mass Spectrometry* **2004**, *233*, 67–73, Special Issue: In honour of Tilmann Mark.

(13) Gutsev, G. L.; Adamowicz, L. The structure of the CF_4 anion and the electron affinity of the CF_4 molecule. *The Journal of Chemical Physics* **1995**, *102*, 9309–9314.

(14) Dobulis, M.; Thompson, M.; Sommerfeld, T.; Jarrold, C. C. Temporary anion states of fluorine substituted benzenes probed by charge transfer in $O_2^-{\cdot}C_6H_{6-x}F_x$ ($x = 0 - 5$) ion-molecule complexes. *J. Chem. Phys.* **204309**, *152*, 2020.

(15) Davis Jr, J. U.; Jarrold, C. C.; Sommerfeld, T. Charge distribution in oxygen·fluorobenzene complex anions $[O_2{\cdot}C_6H_{6-n}F_n]^-$ ($n = 0 - 6$). *Chem. Phys.* **2023**, *574*, 112023.

(16) McGee, C. J.; McGinnis, K. R.; Jarrold, C. C. Anion Photoelectron Imaging Spectroscopy of $C_6HF_5^-$, $C_6F_6^-$, and the Absence of $C_6H_2F_4^-$. *J. Phys. Chem. A* **2023**, *127*, 8556–8565.

(17) Symons, M. C. R. σ^* Radical anions from halogen derivatives of perfluorobenzene. *J. Chem. Soc., Faraday Trans. 1* **1981**, *77*, 783–790.

(18) McGinnis, K. R.; McGee, C. J.; Sommerfeld, T.; Jarrold, C. C. Anion photoelectron imaging spectroscopy of $C_6F_5X^-$ (X = F, Cl, Br, I). *The Journal of Physical Chemistry A* **2024**, *128*, 5646–5658.

(19) Volatron, F.; Roche, C. Electron affinity of perhalogenated benzenes: A theoretical DFT study. *Chemical Physics Letters* **2007**, *446*, 243–249.

(20) Voora, V. K.; Jordan, K. D. Nonvalence correlation-bound anion state of C_6F_6: Doorway to low-energy electron capture. *The Journal of Physical Chemistry A* **2014**, *118*, 7201–7205.

(21) Driver, N.; Jena, P. Electron affinity of modified benzene. *International Journal of Quantum Chemistry* **2018**, *118*, e25504.

(22) Rogers, J. P.; Anstöter, C. S.; Bull, J. N.; Curchod, B. F. E.; Verlet, J. R. R. Photoelectron spectroscopy of the hexafluorobenzene cluster anions: $(C_6F_6)_n^-$ (n = 1–5) and $I^-(C_6F_6)$. *J. Phys. Chem. A* **2019**, *123*, 1602–1612.

(23) Knighton, W. B.; Bognar, J. A.; Grimsrud, E. P. Reactions of selected molecular anions with oxygen. *Journal of Mass Spectrometry* **1995**, *30*, 557–562.

(24) Paran, G. P.; Utku, C.; Jagau, T.-C. On the performance of second-order approximate coupled-cluster singles and doubles

methods for non-valence anions. *Phys. Chem. Chem. Phys.* **2024**, *26*, 1809–1818.

(25) Miller, T. M.; Viggiano, A. A. Electron attachment and detachment: C_6F_5Cl, C_6F_5Br, and C_6F_5I and the electron affinity of C_6F_5Cl. *Phys. Rev. A* **2005**, *71*, 012702.

(26) Nakagawa, S. The branching ratio of anions in thermal electron attachment to chlorinated fluorobenzenes. *International Journal of Mass Spectrometry* **2004**, *235*, 1–5.

(27) Chai, J.-D.; Head-Gordon, M. Systematic optimization of long-range corrected hybrid density functionals. *J. Chem. Phys.* **2008**, *128*, 084106.

(28) Karton, A.; Tarnopolsky, A.; Lamére, J.-F.; Schatz, G. C.; Martin, J. M. L. Highly accurate first-principles benchmark data sets for the parametrization and validation of density functional and other approximate methods. Derivation of a robust, generally applicable, double-hybrid functional for thermochemistry and thermochemical kinetics. *The Journal of Physical Chemistry A* **2008**, *112*, 12868–12886.

(29) Rappoport, D.; Furche, F. Property-optimized Gaussian basis sets for molecular response calculations. *J. Chem. Phys.* **2010**, *133*, 134105.

(30) Ásgeirsson, V.; Birgisson, B. O.; Bjornsson, R.; Becker, U.; Neese, F.; Riplinger, C.; Jónsson, H. Nudged elastic band method for molecular reactions using energy-weighted springs combined with eigenvector following. *Journal of Chemical Theory and Computation* **2021**, *17*, 4929–4945.

(31) Moiseyev, N. *Non-Hermitian quantum mechanics*; Cambridge University Press, Cambridge, UK, 2011.

(32) Davis Jr, J. U.; Sommerfeld, T. Computing resonance energies directly: Method comparison for a model potential. *Eur. Phys. J. D* **2021**, *75*, 316.

(33) Riplinger, C.; Neese, F. An efficient and near linear scaling pair natural orbital based local coupled cluster method. *J. Chem. Phys.* **2013**, *138*, 034106.

(34) Neese, F. The ORCA program system. *Wiley Interdisciplinary Reviews: Computational Molecular Science* **2012**, *2*, 73–78.

(35) Neese, F.; Wennmohs, F.; Becker, U.; Riplinger, C. The ORCA quantum chemistry program package. *The Journal of Chemical Physics* **2020**, *152*, 224108.

(36) Software for the frontiers of quantum chemistry: An overview of developments in the Q-Chem 5 package. *J. Chem. Phys.* **2021**, *155*, 084801.

(37) Gutowski, M.; Skurski, P.; Boldyrev, A. I.; Simons, J.; Jordan, K. D. Contribution of electron correlation to the stability of dipole-bound anionic states. *Phys. Rev. A* **1996**, *54*, 1906.

(38) Sommerfeld, T.; Bhattarai, B.; Vysotskiy, V. P.; Cederbaum, L. S. Correlation-bound anions of NaCl clusters. *J. Chem. Phys.* **2010**, *133*, 114301.

(39) Abdoul-Carime, H.; Desfrançois, C. Electrons weakly bound to molecules by dipolar, quadrupolar or polarisation forces. *Eur. Phys. J. D* **1998**, *2*, 149.

(40) Desfrançois, C. Determination of binding energies of ground-state dipole-bound molecular anions. *Phys. Rev. A* **1995**, *51*, 3667.

(41) Hammer, N. I.; Diri, K.; Jordan, K. D.; Desfrançois, C.; Compton, R. N. Dipole-bound anions of carbonyl, nitrile, and sulfoxide containing molecules. *J. Chem. Phys.* **2003**, *119*, 3650–3660.

(42) Simons, J. Theoretical study of negative molecular ions. *Ann. Rev. Phys. Chem.* **2011**, *62*, 107–128.

(43) Sommerfeld, T.; Davis, M. C. Excluded-volume descriptors for dipole-bound anions: Amine N-oxides as a test case. *J. Chem. Phys.* **2020**, *152*, 054102.

(44) Sommerfeld, T.; Dreux, K. M.; Joshi, R. Excess electrons bound to molecular systems with vanishing dipole but large molecular quadrupole. *J. Phys. Chem. A* **2014**, *118*, 7320–7329.

(45) Voora, V. K.; Kairalapova, A.; Sommerfeld, T.; Jordan, K. D. Theoretical approaches for treating non-valence correlation-bound anions. *J. Chem. Phys.* **2017**, *147*, 214114.

(46) Braïda, B.; Hiberty, P. C. Diatomic halogen anions and related three-electron-bonded anion radicals: Very contrasted performances of Moller-Plesset methods in symmetric vs dissymmetric cases. *J. Phys. Chem. A* **2000**, *104*, 4618.

(47) O'Hagan, D. Understanding organofluorine chemistry. An introduction to the C–F bond. *Chem. Soc. Rev.* **2008**, *37*, 308–319.

TOC Graphic

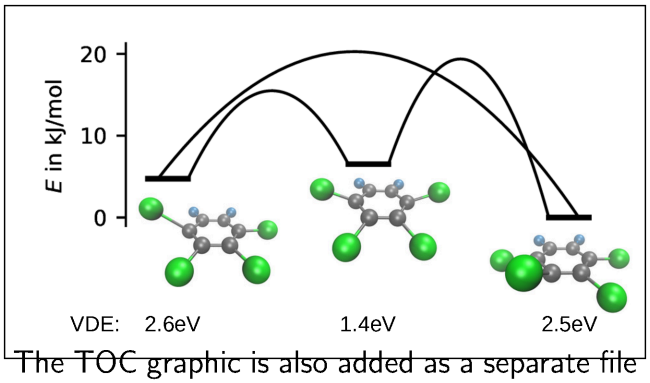

The TOC graphic is also added as a separate file TOC.eps.

The achemso package draws a surrounding frame of 9 cm by 3.5 cm, which is the maximum permitted for *Journal of the American Chemical Society* graphical table of content entries. The box will not resize if the content is too big: instead it will overflow the edge of the box.

The Journal of Physical Chemistry A uses a slighty different size of 3.25 inches by 1.75 inches.